POLYPUBLIE
Polytechnique Montréal

POLYTECHNIQUE MONTRÉAL
UNIVERSITÉ D'INGÉNIERIE

Document en libre accès dans PolyPublie
Open Access document in PolyPublie

Document publié chez l'éditeur officiel
Document issued by the official publisher

Experimental and theoretical assessment of water sorbent kinetics

Authors: Ulrich Legrand [a], Pierre-Luc Girard-Lauriault [b], Jean-Luc Meunier [b], Richard Boudreault [c], Jason Robert Tavares [a]*

Affiliations:

[a] CREPEC, Chemical Engineering Department, Polytechnique Montreal, 2500 Chemin de Polytechnique, Montréal, QC H3T 1J4, Canada

[b] Department of Chemical Engineering, McGill University, 3610 University, Montréal, QC H3A 0C5, Canada

[c] Awn Nanotech, Inc., 1985 55th Ave, Suite 100, Dorval, Qc, H9P 1G9, Canada

*corresponding author email: jason-robert.tavares@polymtl.ca

Abstract: The kinetics of water adsorption in powder sorbent layers are important to design a scaled-up atmospheric water capture device. Herein, the adsorption kinetics of three sorbents, a chromium (Cr) based metal-organic framework (Cr-MIL-101), a carbon-based material (nanoporous sponges/NPS) and silica gel, have been tested experimentally, using powder layers ranging from ~0 to 7.5 mm in thickness, in a custom-made calibrated environmental chamber cycling from 5 to 95 % RH at 30 °C. A mass and energy transfer model was applied on the experimental curves to better understand the contribution of key parameters (maximum water uptake, kinetics of single particles, layer open porosity and particle size distribution). Open porosity (i.e. the void to particle ratio in the sorbent layer) shows the highest influence to improve the kinetics. Converting the sorbent kinetics data into a daily yield of captured water demonstrated (i) the existence of an optimal open porosity for each sorbent, (ii) that thinner layers with moderate open porosity performed respectively better than thicker layers with high open porosity and (iii) that high maximum water uptake and fast single particle kinetics are not necessarily predictive of high daily water yield.

Keywords: kinetics, water capture, sorbents, open porosity, diffusion model

Introduction

It was estimated by the World Health Organization (WHO) in 2019 that 2.2 billion people do not have safely managed drinking water services, while 4.2 billion people lack safely managed sanitation services, i.e. having access to water free of contamination and toilets whose wastes are treated.[1] Improvements were observed between 2000 and 2019 where 1.8 billion people gained access to basic drinking water services, corresponding to a protected water source accessible in less than 30 min, improved toilets and handwashing facilities. These improvements were mostly attributed to better sanitation conditions in third-world countries.[2] Water demand is continuously increasing and has been multiplied by 6 over 100 years due to population increase, economic development and higher consumption.[3] The Organisation for Economic Co-operation and Development (OECD) projected in 2012 that water demand would grow by 55 % between 2000 and 2050.[4]

On top of the already existing water crisis, climate change is likely to exacerbate the situation. Some water-stressed regions such as Middle-East, South Africa, Southwest Asia are expected to become drier, while some regions that currently have abundant water resources could face scarcity.[3] Climate change can act on water supply through many different aspects including extreme weather events, contamination during floods, degradation of ecosystems (forests and wetlands), increasing ocean levels, and melting of the glaciers, among other devastating effects.[5] A larger proportion of water is also contained within the atmosphere with increasing temperature. The development of innovative methods to supply clean and affordable water to populations is consequently of prime importance. One of these methods is already commercially available: water desalination through reverse osmosis (RO).[6] However, RO is limited to locations with access to seawater, generates chemical waste due to the products required for water pre-treatment, produces

2

a super-saturated brine solution that locally depletes oxygen water levels when released in the ocean and requires large amounts of energy, up to 10 $kWh\cdot m^{-3}$ and capitalisation.[7] Alternatively, water can be harvested from atmosphere; it is estimated that 13,000 km^3 of freshwater is stored in the atmosphere and this amount is likely to increase with global warming.[8] Water can be captured under the form of droplets via fog harvesting or vapor with dehumidification techniques.[9]–[11] Dehumidification can be classified as thermodynamics methods, whereby humid air is cooled below dew point and water is condensed and collected;[12] and adsorption methods, where a porous material spontaneously adsorbs water that is later released and condensed.[13] Thermodynamic methods are well-established methods but also require significant energy, up to 550 $kWh\cdot m^{-3}$ of generated water.[14] On the other hand, sorbents have recently gained consideration as vehicles for atmospheric water generation (AWG). An ideal sorbent to capture water at an industrial level would present six important characteristics: high water uptake at low RH, fast adsorption/ desorption kinetics, stability over adsorption/desorption cycles, low energy requirement for desorption, inexpensive production, and potential for scalability. Silica gel is one example of sorbent that is currently employed for dehumidification applications, but suffers from high temperature recovery (more than 100 °C) and degradation of stability over adsorption-desorption cycles.[15]

Recent research has focused on metal-organic frameworks (MOFs), a network of coordinated metal ions and organic ligands in materials with highly controlled properties.[16] Such sorbents can offer narrow pore size distributions targeted towards pore sizes favorable for water adsorption and preventing undesirable hysteresis between the adsorption and desorption. Water uptakes of more than 1 $kg_{water}\cdot kg_{sorbent}^{-1}$ have been observed with these materials,[17] though they are often subject to hydrolytic instability, i. e. degradation of the material due to the presence of water.[18] Also,

3

MOFs require complex, lengthy and costly synthesis processes that make them difficult to scale-up to industrially-relevant levels for water adsorption.[19]

More recently, we reported the synthesis of nanoporous sponges (NPS) based on the pyrolysis of resorcinol-formaldehyde resins.[20] As synthesized, this material can capture 0.15 $kg_{water} \cdot kg_{sorbent}^{-1}$, but when oxidized in post-pyrolysis treatment, water uptake can reach up to 0.20-0.30 $kg_{water} \cdot kg_{sorbent}^{-1}$. While these values are lower than the best performing MOFs or even silica gel, carbon-based sorbents show very strong commercial potential due to their high stability, low production cost, and large potential for production scale-up because of their simple synthesis route. Water uptake at equilibrium however is not the sole point of comparison that should be considered when judging sorbents, kinetics must be taken into account to assess real-world performance. Studies on sorbents for water capture generally report experimental kinetics data that cannot be directly compared to others. Indeed, several parameters outside of the nature of the sorbent itself have an important role in the adsorption kinetics and are not always reported in literature, for example: (a) the sorbent particle size distribution will dictate the water intra-particle diffusion, (b) the sorbent open porosity influences the water inter-particle diffusion, and (c) the sorbent powder layer thickness will affect diffusion and thus adsorption kinetics. In this regard, we differ from literature generally reporting only maximum water uptake, i.e. the maximum amount of water that can be adsorbed by a specific sorbent. Instead, we report this value along with daily water yield (DWY) of a sorbent layer having a specific thickness. The DWY corresponds to the amount of water delivered by this sorbent layer through adsorption-desorption cycles over a 24h period, and thus presents a value more representative of actual use in a water capture device. Herein, we experimentally and theoretically study the kinetics of several representative sorbents: NPS, silica gel, and a high-performance chromium-based MOF, namely Cr-MIL-101.

Materials and methods

Sorbent materials

The NPS are synthesized from the pyrolysis of resorcinol-formaldehyde resin, a procedure described thoroughly in Legrand *et al.*[20] Type A silica gel (Dry-Packs®) was purchased from Amazon. Common silica gel (used as a desiccant) was selected over research grades since large-scale applications are more likely to employ a widely available and inexpensive product. Cr-MIL-101 is a chromium-based MOF that has already been described is literature and was purchased from Nanoshel-UK LTD.[22], [23]

Environmental chamber

The kinetics of each sorbent were assessed by a gravimetric method in a custom-made environmental chamber shown in Figure S1. Both a humidifier and dry air injection regulate the air humidity from 5 to 95 % RH, while a heater controls the temperature from ambient to 38 °C. The air is homogenized in the environmental chamber with a fan. The humidity, temperature and fan controls were managed with an Arduino Uno R3 via a computer interface. The powder sample is placed in a glass dish with known diameter, suspended under a AB204-S analytical balance from Mettler Toledo. The mass change of the sorbent sample is recorded in real-time. Samples underwent drying steps at 30 °C and minimal RH in the environmental chamber for durations dependent on the layer thickness (4 h for minimal thickness and up to 24 h for 7.5 mm layer) prior to the humidity being changed to 95 % RH. This step was maintained until the mass change reached an equilibrium corresponding to the sorbent water saturation. The drying step was then repeated to empty the sorbents and ensure an appropriate baseline. The thickness of the sorbent powder layer was selected at 1, 2, 3 and 7.5 mm, as well as a test with minimal thickness (~0 mm). The layer thickness was varied by changing the sorbent mass in a glass dish with known surface area,

while knowing the sorbent apparent density. For minimal thickness, a glass dish with surface area of 71 cm^2 was selected with less than 500 mg of sorbent. The tests with higher thicknesses were performed in a smaller glass dish with a surface area of 16 cm^2 to limit the used powder. Layers of 7.5 mm respectively used 9.7, 9.4 and 3.2 g of dried silica gel, NPS and Cr-MIL-101. Increasing the humidity from 5 to 95 % RH in the environmental chamber was not instantaneous and required an average duration of 800 s for the humidity to equilibrate. The kinetics data were thus corrected to take this effect into account. Temperature evolution of the sorbents was performed with a flat thermocouple sitting at the bottom of the powder layer and separated from the sorbent with a piece of aluminum foil.

Mass and energy transport in a sorbent layer

The adsorption kinetics are studied experimentally and can be modelled assuming spherical particles of known radius using Fick's law of diffusion (Equation 1), that the full derivation is well-developed in the supplementary information from Kim *et al.*[21]

$$\frac{\partial C}{\partial t} = \frac{1}{r_c^2} \frac{\partial}{\partial r}\left(D_\mu r_c^2 \frac{\partial C}{\partial r}\right) \qquad \text{(Equation 1)}$$

where C is the airborne water vapor concentration within the packed adsorbent layer [mol·m^{-3}], r_c is the particle radius [m], and D_μ is the intra-particle diffusion coefficient [m^2·s^{-1}]. A mathematical solution of Fick's law was used in a way to introduce actual gravimetric data (Equation 2).[24]

$$\frac{m_t}{m_{eq}} = 1 - \frac{6}{\pi^2} \sum_{n=1}^{\infty} \left(\frac{1}{n^2}\right) e^{\left(-\frac{n^2\pi^2 D_\mu t}{r_c^2}\right)} \qquad \text{(Equation 2)}$$

In Equation 2, m_t represents the mass of adsorbed water in the sorbent particle at time t, and reaches an equilibrium value m_{eq} after a sufficiently long time. m_t/m_{eq} refers to the fractional water uptake (FWU), a gravimetric parameter describing adsorption being equal to 0 at $t = 0$ s, and equal to 1 once the equilibrium water uptake has been reached. The intra-particle diffusion coefficient can be determined over a range of relative humidity and temperature. Once determined, a simple kinetics profile based on the linear driving force model (Equation 3) can predict the adsorption or desorption rate over time.[25]

$$\frac{\partial C_\mu}{\partial t} = \frac{15}{r_c^2} D_\mu \left(C_{eq} - C_\mu \right) \qquad \text{(Equation 3)}$$

where C_μ is the instantaneous vapor concentration in the particle [mol/m³], and C_{eq} is the equilibrium vapor concentration [mol·m⁻³]. The solution to the linear driving force model is provided in Equation 4.

$$\frac{m_t}{m_{eq}} = 1 - e^{-k_L t} \qquad \text{(Equation 4)}$$

where m_t/m_{eq} corresponds to a simpler FWU profile and k_L [s⁻¹] corresponds to $15D_\mu/r_c^2$.

With these equations as a starting point, the model described in detail by Kim *et al.*[21] is applied and solved for the present case. Specifically, it consists of the equations of mass and energy transport in a packed adsorbent layer of known thickness (Equations 5 and 6). This model takes into account the water vapour diffusion between the particles (inter-particle diffusion) and the ability of the particles to adsorb and retain water (intra-particle diffusion).

$$\frac{\partial C}{\partial t} = \nabla \cdot D_v \nabla C - \frac{(1-\varepsilon)}{\varepsilon} \frac{\partial C_\mu}{\partial t} \qquad \text{(Equation 5)}$$

$$\rho c_p \frac{\partial T}{\partial t} = \nabla \cdot k \nabla T + h_{ad}(1-\varepsilon)\frac{\partial C_\mu}{\partial t} \qquad \text{(Equation 6)}$$

where C is the airborne water vapor concentration within the packed adsorbent layer [mol·m⁻³], T is the temperature in the packed adsorbent [K], D_v is the inter-particle diffusion coefficient [m²·s⁻¹], ε is the packed porosity, $\partial C_\mu/\partial t$ is the adsorption/desorption rate provided by the gravimetric data [mol·m⁻³·s⁻¹], ρ is the locally averaged volumetric density [kg·m⁻³], c_p is the specific heat capacity of the adsorbent [J·K⁻¹·kg⁻¹], k is the thermal conductivity [W·m⁻¹·s⁻¹] and h_{ad} is the enthalpy of adsorption [J·mol⁻¹]. The inter-particle diffusion coefficient D_v is determined by the methodology detailed in the Supplementary Information (Equations S1-S5). The adsorption rate $\partial C_\mu/\partial t$ was replaced with the linear driving force model given by Equation 3, where C_{eq}, the equilibrium vapor concentration at a given water partial pressure [mol·m⁻³], was extrapolated from each isotherm at 30 °C.

Mass and energy transfer equations were solved using the finite difference method; the methodology is detailed in Supplementary Information (Equations S6-S13, Figure S2). Both mass and energy transfer equations were solved independently from each other. The temperature dependence of parameters such as D_v was neglected in the present case since temperature measurements showed no important increase during the experiments. Such uniform temperature resulted from low powder layer thicknesses and constant temperature being maintained in the environmental chamber. The temperature measurements of 2 mm layers for the studied sorbents are shown in Figure S3 to confirm this assumption. Interparticle diffusion varied by less than 0.1 % when the temperature was varied by 10 K for the studied sorbents.

Physical characterization of the sorbents

The open porosity was measured experimentally following Equation 7.

$$\varepsilon = 1 - \frac{\rho_{ads}}{\rho_{powder}} \qquad \text{(Equation 7)}$$

where ρ_{ads} is the apparent density of the adsorption layer [kg·m^{-3}] and ρ_{powder} is the absolute density of the particles [kg·m^{-3}]. The value of ρ_{ads} was determined by weighing a known volume of adsorbent with a precision balance, and ρ_{powder} was measured on an AccuPyc II 1340 gas pycnometer under helium atmosphere. One should note that the minimum packing porosity for spherical particles (0.25) is obtained for hexagonal closed-packed configuration. The sorbent particle size was separately measured for volume and number distribution. Volume distribution measurement was performed by dynamic light scattering (DLS) on a Malvern Mastersizer 3000 while diameter distribution was measured with laser particle sizer (LPS) on an EyeTech from Ankersmid. LPS employs a rotating laser beam to measure the duration of obscuration and deduce particle size. As such, this method can directly provide a number distribution, but it is not sensitive for diameters smaller than 0.1 μm, and thus not applied to the Cr-MIL-101 sample whose manufacturer specifies sizes comprised in the 30 – 50 nm range.

Results and Discussion

Theoretical vs experimental adsorption kinetics

Kinetics of sorbent layers depend on the nature of the sorbent itself, but also on several characteristics including the maximum water uptake, open porosity, particle size distribution and adsorption kinetics for single particles. The maximum water uptake at 30°C was determined from the adsorption isotherms of Cr-MIL-101, silica gel and NPS (Figure 1). The sorbent's particle size distribution, measured separately for number and volume distribution, are shown in Figures S4 and S5. Silica gel and NPS exhibited highly polydisperse characteristics contrary to Cr-MIL-101's narrower distribution. One should note that the Cr-MIL-101 volume distribution was measured up

to 1 µm due to the presence of agglomerates in the water suspension. Agglomerates were likely also present in the powder layer due to the tendency of nanoparticles to naturally agglomerate,[26] but their contribution was implicitly taken into account when calculating the layer open porosity. As such, the diffusion properties for Cr-MIL-101 were calculated for an average particle size of 40 nm. All of the sorbent characteristics are summarized in Table 1 for the three tested samples.
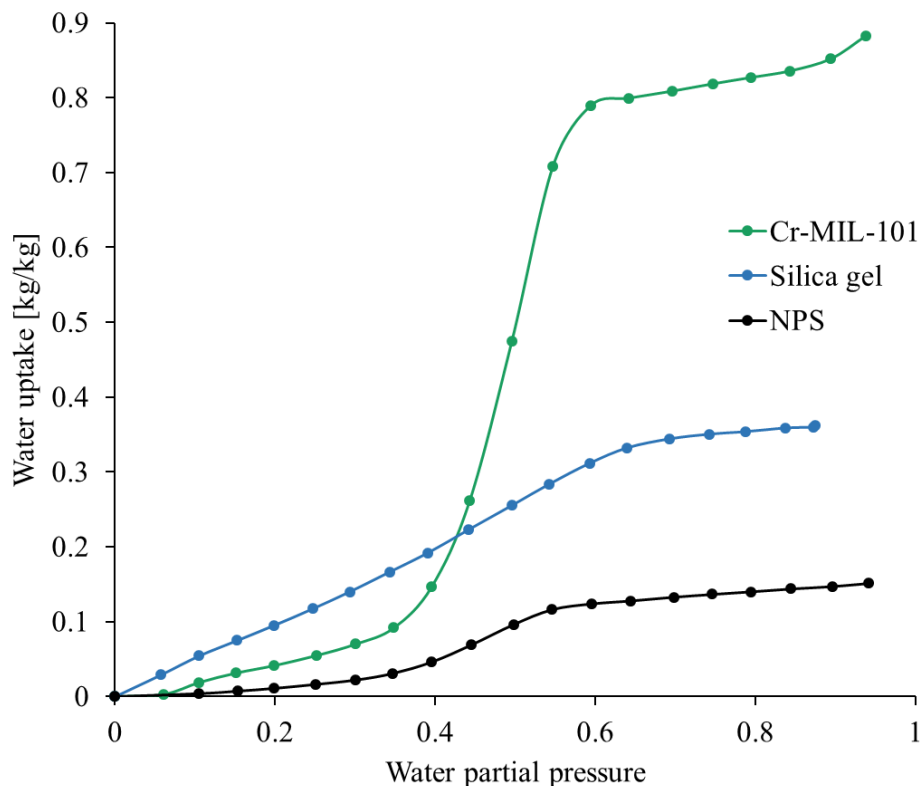

Figure 1: Adsorption isotherms of Cr-MIL-101, silica gel and NPS measured at 30°C.

Table 1: Summary of the sorbent characteristics.

Sorbent	Cr-MIL-101	Silica gel	NPS
Maximum water uptake ($kg_{water} \cdot kg_{sorbent}^{-1}$)	0.87	0.36	0.15
Open porosity	0.82	0.57	0.51
Particle size distribution	30-50 nm	From <1 µm to >100 µm	From <1 µm to >100 µm

Time to reach 90% of maximum water for ~0 mm layer (s)	689	504	1183

The experimental adsorption kinetics curves for the various thicknesses are summarized in Figure S6. As expected, the adsorption kinetics are slower for larger layer thicknesses as interparticle diffusion imposes longer times for water vapor to travel from the surface of the layer to its bottom. The adsorption kinetics for thick sorbent layers differed from the adsorption kinetics at ~0 mm (silica gel > Cr-MIL-101 > NPS), where the particles were separated enough to neglect the interparticle diffusion contribution. Indeed, the silica gel had the fastest kinetics at ~0 mm while Cr-MIL-101 had faster kinetics for the thicker layers. As such, determining the kinetics for dispersed sorbent particles in limited quantities cannot be used as a prediction of kinetics in a thicker layer, and thus in a larger water capture system.

To better understand the effects of the sorbent characteristics on their kinetics, the mass transfer model has been applied, with several assumptions. One of these assumptions concerns the particle size distribution: silica gel and NPS exhibit polydisperse particle size distribution with sizes ranging from below 1 μm to higher than 100 μm. However, the model considers monodisperse and spherical particles to determine intra and interparticle diffusion coefficients. It has been assumed that the largest particles have a higher contribution towards intraparticle diffusion while the smallest particles provide a higher contribution towards interparticle diffusion. Indeed, larger particles have the slowest adsorption rate (see Equation 3) and the highest volumetric contribution. Regarding the interparticle diffusion, a polydisperse powder generates more tortuosity for water vapor diffusion through the layer,[27] as illustrated in Figure 2 where the smallest particle occupy the void between larger particles, thus decreasing the characteristic void size between two particles.
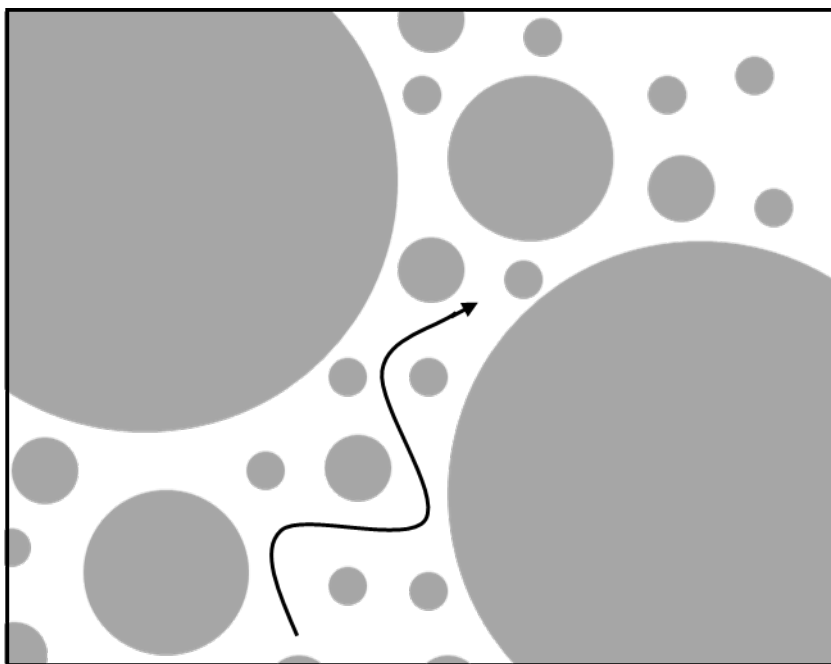
11

Figure 2: Schematic of the more complex inter-particle diffusion in polydisperse particles.

When applying the theoretical model to the experimental data, a large discrepancy was observed for thinner layers with the model predicting faster kinetics than observed while a good adequacy for thicker layer of 7.5 mm was obtained (see Figure S7). Several reasons explaining this discrepancy were proposed including experimental error on the powder layer thickness, where variations of ±1 mm could be observed in the powder layers. However, this was not sufficient to explain the differences between the theoretical curve and experimental data. The retained explanation came from the inadequate boundary layer condition in the theoretical model. Indeed, the model does not account for local water vapor depletion at the surface of the powder layer; such depletion can be explained by the presence of a boundary layer on top of the surface of the powder, as well as walls slowing down the water diffusion from the ambient air to the sorbent surface. The boundary layer is formed when a fluid is moving tangentially to a surface.[28] Considering an extreme case of a flat surface and a low air velocity of 0.15 m·s⁻¹ delivered by the fan in the

environmental chamber, the boundary layer could be between 0.3 and 0.6 mm. This may be an overestimate, given that the presence of walls around the powder probably generated turbulences that can shrink the boundary layer. These walls, having a height of about 3 cm (Figure S1), could also create a zone of depletion in the case of water being adsorbed faster than the diffusion rate in the glass dish. As a reminder, the model utilized a step function to pass from minimum to maximum relative humidity. Consequently, the thinnest layers having the fastest kinetics would be more affected by depletion compared to the largest layer with slower kinetics. The appropriate boundary layer condition at the sorbent layer should then be represented by an exponential profile, where water vapor depletion was less important when the adsorption kinetics became slower, as illustrated in Figure S8. Due to the complexity of the cumulated phenomena, an empirical correction of the theoretical curves at lower thickness was applied under the form of an exponential factor $(1-e^{-\alpha t})$, where α was dependent on the layer thickness. The summary of the experimental and corrected theoretical adsorption kinetics is shown in Figure 3, while the values of the parameters α were given in Table S1.
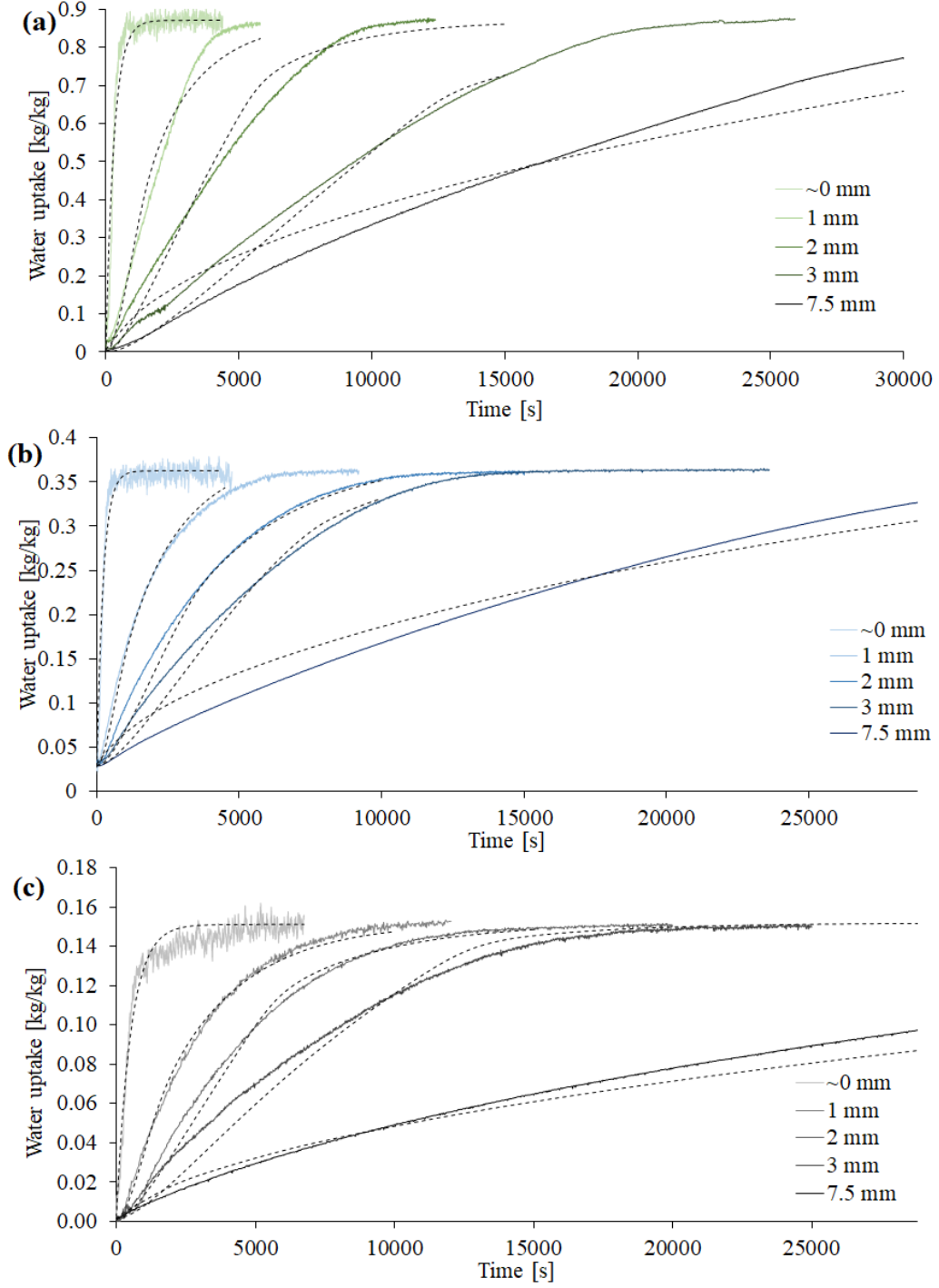
Figure 3: Experimental (full lines) and corrected (dashed lines) theoretical adsorption kinetics for (a) Cr-MIL-101, (b) silica gel and (c) NPS at different thicknesses. Intraparticle diffusion coefficient kL remained constant for the different layer thicknesses and was equal to $k_{L,NPS} = 3.0 \times 10^{-3}$ s^{-1} ; $k_{L,Silica} = 2.1 \times 10^{-3}$ s^{-1} ; $k_{L,Cr-MIL-101} = 3.3 \times 10^{-1}$ s^{-1}.

On top of the theoretical model validation with experimental data, these results were employed to optimize kinetics and provide insight for the design of large-scale water capture system. The model made evident that some parameters had a higher effect at various thicknesses. For example, at the larger studied thickness, it was showed that increasing open porosity had a higher effect compared to decreasing particle size. Indeed, at this larger thickness, limitations are caused by the interparticle diffusion and not by the particle adsorption itself. Increasing the open porosity directly improved the interparticle diffusion, which is further detailed in the following section. For a given open porosity, decreasing the particle size had a more complex effect since it simultaneously improved the intraparticle diffusion while decreasing the interparticle diffusion.

Kinetics for daily water yield determination

A large-scale water capture system based on adsorption/desorption cycles is likely to have layers of powders stacked in a chamber, where humid air is passed over the surface during the adsorption and then is replaced with dry air and/or heat during the desorption. Several designs have been considered in the literature and share similar characteristics of parallel trays with thin layers of sorbent dispersed on them.[12], [13], [29]

As illustrated in Figure 3, a difference of several mm in the layer thickness was observed to cause the adsorption to take several more hours longer. As such, for a given layer thickness of 2 and 7.5 mm, the open porosity was swept from its measured value and up to 0.99 for the three sorbents studied in the model. As shown in Figure S9 for a layer thickness of 7.5 mm, increasing the open porosity caused the kinetics to converge towards the ~0 mm case, where interparticle diffusion could be neglected. Practically, the open porosity can be increased by dispersing the sorbent powder in a macroporous solid structure. For example, Kim et al. employed a copper foam to disperse their MOF powder and thus increase its open porosity, while also increasing heat

15

dissipation during adsorption.[30] However, heat-conductive polymers, such as conjugated polymers,[31] could eventually replace the more expensive copper foam.

Applying some simplifying assumptions, the adsorption kinetics were translated into a daily water yield (DWY) for a specific surface area of sorbent powder of a known thickness (Figure 4). Specifically, it was assumed that the desorption kinetics are similar to the adsorption kinetics, which is generally true for sorbents presenting low hysteresis between adsorption and desorption, such as the NPS. Also, an adsorption step was considered complete when 90% of the maximum water uptake was reached. The detailed calculation to obtain DWY from the kinetics data is presented in Table S2-S4 for a 7.5 mm layer of the different sorbents.
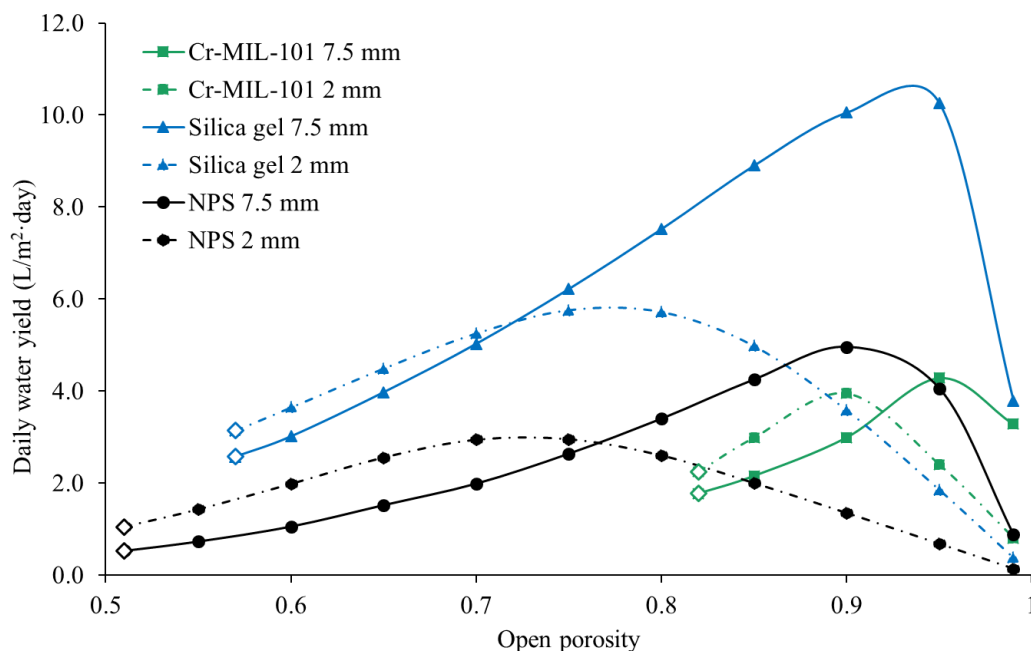

Figure 4: Daily water yield for the three studied sorbents at 2 and 7.5 mm thickness. The diamond-shaped data point for each curve corresponds to the DWY for the measured open porosity.

Converting kinetics into DWY enabled interesting and counter-intuitive observations for the design of large-scale systems. Indeed, it was shown that the sorbent with higher water uptake, i.e.

Cr-MIL-101, did not provide the highest daily yield for all layer thicknesses. Additionally, NPS that have a maximum water uptake nearly 6 times lower than Cr-MIL-101 had a higher DWY for the 7.5 mm layer thickness. This phenomenon was mostly due to the higher apparent density for NPS compared to Cr-MIL-101. Silica gel was the sorbent with the highest water yield for both thicknesses due to faster kinetics coupled with higher apparent density (see Tables S1-S3). It was observed that thin layers, with moderate open porosity, were preferential compared to thicker layer with open porosity closer to 1. However, silica gel is generally not seen as a suitable candidate for large-scale water capture due to high temperature regeneration and material degradation over time. One should note that when increasing the open porosity of a sorbent for a given thickness, the adsorption kinetics are increased while the hypothesis of solving separately the mass transfer from the energy transfer in the theoretical model still holds. The maximum temperature increase was calculated from the energy transfer equation (equation 6) for silica gel, whose thermal properties are available in literature and summarized in Table 2. Consistent thermodynamic characterization of the sorbents was recently realized based on adsorption isotherms at different temperatures.[32] As seen in Figure 5, increasing the open porosity for a layer with constant thickness effectively increases the maximum temperature at the bottom of such layer by up to 37 °C. This was hypothetically caused by a reduction of the layer thermal conductivity with higher open porosity, together with the energy being released over shorter time durations because of the faster kinetics. The intraparticle diffusion varied by less than 0.1% when the temperature was increased from 30 to 37 °C.

Table 2: Summary of thermal properties for silica gel valid at 300 K, from literature.

Thermal property	Value
Enthalpy of adsorption (J·mol^{-1})	50,400 [33]

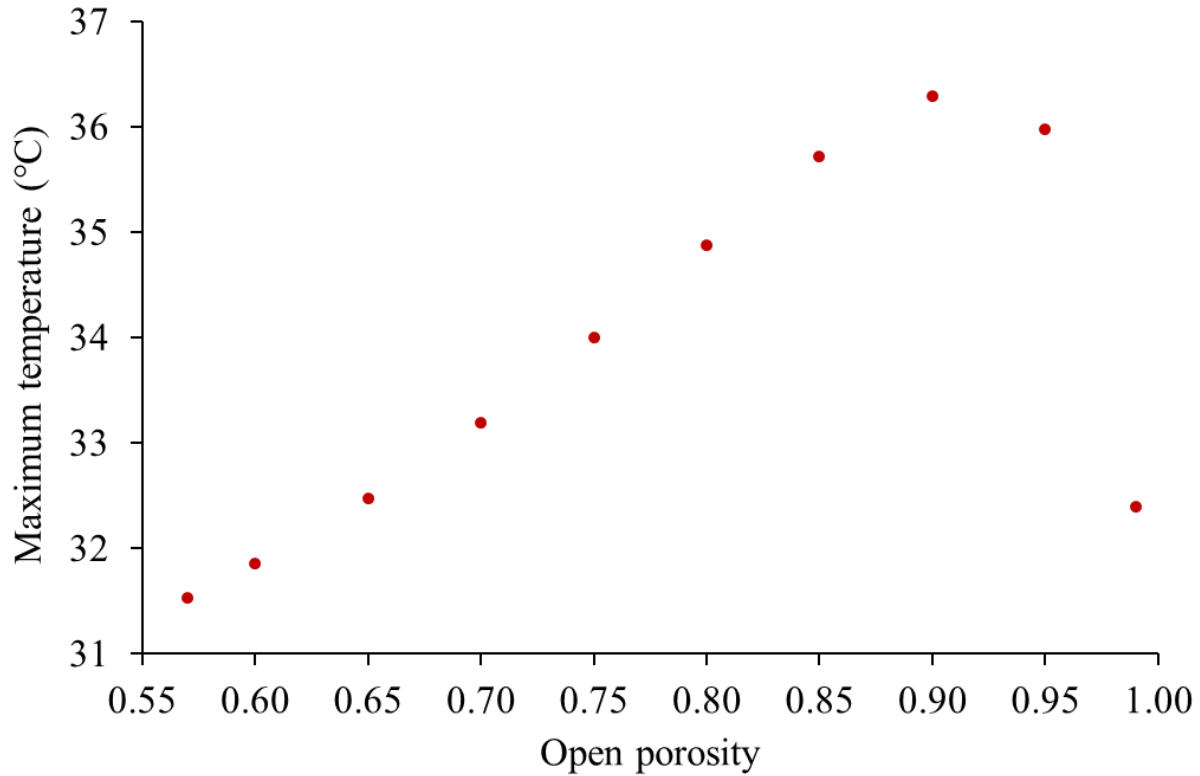| Thermal conductivity (W·m^{-1}·K^{-1})	0.16 [34]
Specific heat capacity (J·K^{-1}·kg^{-1})	850 [35]

Figure 5: Maximum theoretical temperature reached at the bottom of a 7.5 mm silica gel layer depending on the open porosity.

Kinetics for water capture design optimization

Silica gel exhibited the optimal conditions in terms of kinetics, namely a moderate open porosity and high hydrophilicity leading to high intraparticle diffusion. As such, the highest DWY observed for the three studied sorbents was obtained with silica gel. However, some drawbacks would prevent the utilization of silica gel in large-scale water capture set-ups, including a larger hysteresis between the adsorption and desorption that could provoke lower desorption rates, and more importantly a high regeneration temperature (>100 °C). Also, silica gel exhibits documented

degradation that would diminish the material performance over time. This degradation is caused by the dehydroxylation of the silica surface.[15]

Cr-MIL-101 had the highest open porosity and highest water uptake with nanometric particle size. This high open porosity lead to the fastest kinetics at larger layer thickness. It would have been expected that the kinetics of the ~0 mm layer to be faster due to the nanometric particle size. However, these kinetics were probably slowed down due to agglomerates formation. Despite these characteristics, Cr-MIL-101 obtained lower DWY. It is believed that micrometric particles with moderate open porosity, similar to NPS and silica gel, would have led to higher DWYs. However, the size polydispersity of NPS and silica gel probably represented a disadvantage as the smallest particles contributed to a higher layer diffusion resistance, while the adsorption kinetics were still dominated by the largest particles. The optimal particle size distribution would be monodispersed sorbent microparticles at the open porosity maximizing DWY. While silica gel use is widely spread in many commercial applications, Cr-MIL-101 is still a material in research and development that faces scale-up challenges. Efforts to reduce energy and cost requirements are currently undergoing in the field of MOF synthesis scale-up with initiatives like microwave assistance.[36]

Compared to the silica gel and Cr-MIL-101, the NPS exhibited the lowest water uptake and lower kinetics due to a high hydrophobicity of a material made of >90 wt% of carbon. Despite these unfavorable properties, NPS was able to compete in terms of DWY because of a higher apparent density enabling to pack more material in the same layer thickness and open porosity. On top of that, the water uptake of 0.15 $kg_{water}/kg_{sorbent}$ can be improved by post-pyrolysis functionalization with thermal oxidation leading to a water uptake comprised between 0.20 and 0.30 $kg_{water} \cdot kg_{sorbent}^{-1}$.[20] This water uptake could be potentially improved up to 0.50 $kg_{water} \cdot kg_{sorbent}^{-1}$,

as demonstrated Huber *et al.* with a CO_2 activation that drastically improved the microporosity of an initial resorcinol-melamine-formaldehyde resin.[37]

The design of a large-scale system would require accounting for energy transfer due to larger sorbent amounts and more confined spaces, promoting heat accumulation. In the environmental chamber, the temperature was maintained constant at 30 °C and temperature rise at the bottom of the sorbent layers were limited below 10 °C, with the lowest temperature rise observed for NPS (this material has a higher thermal conductivity owing to its carbon composition, enabling it to dissipate heat better than silica gel and Cr-MIL-101). Heat management in a larger system where the temperature is not maintained constant was studied previously. For example, LaPotin *et al.* designed a dual system with separated compartments where the heat of adsorption of one compartment was transferred to the neighbouring compartment in order to perform the desorption step.[38] Using a commercial sorbent (AQSOA Z01) and natural sunlight to provide heat, they obtained a DWY of 0.77 $L \cdot m^{-2} \cdot day^{-1}$. LaPotin *et al.* also utilized a copper foam with high thermal conductivity in which the MOF-801 sorbent was dispersed to enhance heat dissipation.[39]

As mentioned earlier, due to the multi-parametric dependence of the sorbent kinetics, it is difficult to perform comparison between studies found in the literature, but pertinent information can still be gathered.

Van Heyden *et al.* described kinetics layers of aluminophosphate for heat pump applications.[40] They studied thin layers bonded with a polymer (polyvinyl alcohol) from 80 to 760 μm with two types of particles: monodisperse nanoparticles (250 nm) and polydisperse microparticles (0.3 to 3 μm). They concluded that layers with nanoparticles had higher kinetics due to the heat transfer limitations occurring in layers with microparticles. However, they noticed that nanoparticles had a tendency to agglomerate and generate larger void spaces. The open porosity was not clearly

defined, and the layer density appeared variable from a sample to another. It can be supposed from their data that, similarly to the Cr-MIL-101 sample, a higher open porosity and lower particle size improved the adsorption kinetics.

Hanikel *et al.* tested kinetics of their aluminum-based MOF, MOF-303, and compared it to three commercial aluminum-based sorbents, Zeolite 13X, SAPO-34 and Basolite A520.[41] They decided to fix all of the layer parameters for the sorbents (thickness = 3 mm, open porosity = 0.7, particle size distribution = 2-5 μm) in order to determine the effect of the sorbent nature. They determined that their MOF-303 had faster kinetics at 40 % RH compared to the three commercial sorbents, but the reason for these faster kinetics was unclear. They supposed that MOF-303 had a higher hydrophilic nature than their counterparts. More importantly, they concluded that the water uptake of a sorbent at a given RH cannot predict its adsorption rate.

Hossain *et al.* measured the kinetics on a pellet fragment of UiO-66 MOF using a concentration-swing frequency response (CSFR) device at various RH.[42] With an S-shape isotherm similar to NPS and Cr-MIL-101 and corresponding to hydrophobic behavior, they determined that the water adsorption rate was not constant over the RH range and presented a minimum at the inflexion point of the S-shaped isotherm. This study showed that kinetics were also dependent on the surrounding RH. While we worked on the kinetics at high RH, it would still be pertinent to perform a similar comparison at lower RH.

Conclusion

Based on experimental and theoretical study of the adsorption kinetics of three sorbents (Cr-MIL-101, silica gel, NPS), it was possible to demonstrate that kinetics were mostly influenced by the sorbent layer open porosity. Larger open porosity decreased the contribution of the interparticle diffusion allowing to improve the layer kinetics. When calculating the DWY with layers of

variable theoretical open porosity, it was shown that silica gel obtained the highest performance. NPS, with a maximum water uptake nearly 6 times lower than Cr-MIL-101, still obtained higher DWY for the 7.5 mm layer. A higher apparent density, enabling to pack more sorbent for the same thickness and compensating for the lower water uptake, explained this phenomenon. From this research, several experimental pathways are envisioned to continue the optimization of sorbent layers kinetics. The experimental set-up could be modified to prevent water vapor depletion in the glass dish by lowering the walls near the surface of the sorbent layers. It would help the model to better fit the experimental curves. While the adsorption kinetics have been measured at maximum RH, it would also be pertinent to study kinetics and DWY in function of the RH. Since the open porosity appeared to be an important factor in optimizing both kinetics and DWY, the study of metallic or polymer foams with various levels of macroporosity is primordial in the design of optimal sorbent layers. Beyond the layers themselves, a scaled-up atmospheric water capture device based on parallel sorbent layers can further be optimized for several parameters including the layers' spacing, humid air flow rate, heat management, and others.

Supporting Information

Additional information on the experimental set-up, details on the calculation of the inter-particle coefficients, resolution of the finite difference method, additional characterization analyses and data tables.

Acknowledgements

from Polytechnique Montreal for respectively helping us to perform pycnometer, laser particle sizer and dynamic light scattering measurements on our samples. We would like to thank Sean Watson from Polytechnique Montreal for his help on the automation aspect of our environmental chamber, as well as Prof. Michael R. Wertheimer for his collaboration and point of view on the project.

Conflict of interest

References

[1]   Osseiran, N. and Lufadeju, Y. UNICEF, WHO Credits 1 in 3 people globally do not have access to safe drinking water – UNICEF, WHO, 2019. https://www.who.int/news/item/18-06-2019-1-in-3-people-globally-do-not-have-access-to-safe-drinking-water-unicef-who (accessed Jun. 29, 2021).

[2]   Pickford, J. Sustainable Water Supply and Improved Sanitation for Low Income Communities. Technology and Developing Countries, 1995, 3.

[3]   Chang, H. Water and Climate Change. 2019.

[4]   Organization for economic co-operation and development, Environmental Outlook to 2050: The consequences of Inaction. 2012.

[5]   Shukla, P. R.; Skea, J.; Buendia, E. C.; Masson-Delmotte, V.; Pörtner, H.-O.; Roberts, D. C.; Zhai, P.; Slade, R.; Connors, S.; Van Diemen, R.; Ferrat, M.; Haughey, E.; Luz, S.; Neogi, S.; Pathak, M.; Petzold, J.; Pereira, J. P.; Vyas, P.; Huntley, E.; Kissick, K.; Belkacemi, M.; Malley, J. IPCC, 2019: Climate Change and Land: an IPCC special report on climate change, desertification, land degradation, sustainable land management, food security, and greenhouse gas fluxes in terrestrial ecosystems. 2019.

[6]   Zotalis, K.; Dialynas, E. G.; Mamassis, N.; Angelakis, A. N. Desalination technologies: Hellenic experience. Water (Switzerland), 6, 5, 1134–1150, 2014.

[7]   Terry, C. The Disadvantages of Desalination. 2021. https://sciencing.com/pros-cons-of-desalination-plants-13425360.html (accessed Jul. 20, 2021).

[8]   Gleick, P. H. Water resources. Encyclopedia of Climate and Weather, Oxford Uni., S. H. Schneider, Ed. 1996, 817–823.

[9]   Klemm O.; Schemenauer, R. S.; Lummerich, A.; Cereceda, P.; Marzol, V.; Corell, D.; Van Heerden, J.; Reinhard, D.; Gherezghiher, T.; Olivier, J.; Osses, P.; Sarsour, J.; Frost, E.; Estrela, M. J.; Valiente, J. A.; Fessehaye, G. M. Fog as a fresh-water resource: Overview and perspectives. Ambio, 41, 3, 221–234, 2012.

[10]   Fessehaye, M.; Abdul-Wahab, S. A.; Savage, M. J.; Kohler, T.; Gherezghiher, T.; Hurni, H. Fog-water collection for community use. Renew. Sustain. Energy Rev., 29, 52–62, 2014.

[11]   Shi, W.; Anderson, M. J.; Tulkoff, J. B.; Kennedy, B. S.; Boreyko, J. B. Fog Harvesting with Harps. ACS Appl. Mater. Interfaces, 10, 14, 11979–11986, 2018.

[12]   Tu, Y.; Wang, R.; Zhang, Y.; Wang, J. Progress and Expectation of Atmospheric Water Harvesting. Joule, 2, 8, 1452–1475, 2018.

[13]   Zhou, X.; Lu, H.; Zhao, F.; Yu, G. Atmospheric Water Harvesting : A Review of Material and Structural Designs. ACS Mater. Lett., 2, 671–684, 2020.

[14]   Wahlgren, R. V. Atmospheric water vapour processor designs for potable water production: A review. Water Res., 35, 1, 1–22, 2001.

[15]   Wang, D.; Zhang, J.; Xia, Y.; Han, Y.; Wang, S. Investigation of adsorption performance deterioration in silica gel-water adsorption refrigeration. Energy Convers. Manag., 58, 157–162, 2012.

[16]   Canivet, J.; Fateeva, A.; Guo, Y.; Coasne, B.; Farrusseng, D. Water adsorption in MOFs: Fundamentals and applications. Chem. Soc. Rev., 43, 16, 5594–5617, 2014.

[17]   Kalmutzki, M. J.; Diercks, C. S.; Yaghi, O. M. Metal–Organic Frameworks for Water Harvesting from Air. Adv. Mater., 30, 37, 1–26, 2018.

[18]   Gelfand, B. S.; Shimizu, G. K. H. Parameterizing and grading hydrolytic stability in metal-organic frameworks. Dalt. Trans., 45, 9, 3668–3678, 2016.

[19]   Rubio-Martinez, M.; Avci-Camur, C.; Thornton, A. W.; Imaz, I.; Maspoch, D.; Hill, M. R. New synthetic routes towards MOF production at scale. Chem. Soc. Rev., 46, 11, 3453–3480, 2017.

[20]   Legrand, U. Klassen, D.; Watson, S.; Aufoujal, A.; Nisol, B.; Boudreault, R.; Waters, K. E.; Meunier, J.-L.; Girard-Lauriault, P.-L.; Wertheimer, M. R.; Tavares, J. R. Nanoporous

sponges as carbon-based sorbents for atmospheric water generation. Ind. Eng. Chem. Res. 60, 35, 12923-12933, 2021.

[21]   Hyunho, K.; Yang, S.; Rao, S. R.; Narayanan, S.; Kapustin, E. A.; Furukawa, H.; Umans, A. S.; Yaghi, O. M.; Wang, E. N. Water harvesting from air with metal-organic frameworks powered by natural sunlight. Science, 356, 6336, 430–434, 2017.

[22]   Tan, B.; Luo, Y.; Liang, X.; Wang, S.; Gao, X.; Zhang, Z.; Fang, Y. Mixed-Solvothermal Synthesis of MIL-101(Cr) and Its Water Adsorption/Desorption Performance. Ind. Eng. Chem. Res., 58, 8, 2983–2990, 2019.

[23]   Ko, N.; Choi, P. G.; Hong, J.; Yeo, M.; Sung, S.; Cordova, K. E.; Park, H. J.; Yang, J. K.; Kim, J. Tailoring the water adsorption properties of MIL-101 metal-organic frameworks by partial functionalization. J. Mater. Chem. A, 3, 5, 2057–2064, 2015.

[24]   Crank, J. The Mathematics of Diffusion, Second Ed. 1975.

[25]   Sircar, S.; Hufton, J. R. Why does the linear driving force model for adsorption kinetics work? Adsorption, 6, 2, 137–147, 2000.

[26]   Ashraf, M. A.; Peng, W.; Zare, Y.; Rhee, K. Y. Effects of Size and Aggregation/Agglomeration of Nanoparticles on the Interfacial/Interphase Properties and Tensile Strength of Polymer Nanocomposites. Nanoscale Res. Lett., 13, 2018.

[27]   Kovalev, O. B.; Gusarov, A. V.; Belyaev, V. V. Morphology of random packing of micro-particles and its effect on the absorption of laser radiation during selective melting of powders. Int. J. Eng. Sci., 157, 103378, 2020.

[28]   Dhawan, S.; Narasimha, R. Some properties of boundary layer flow during the transition from laminar to turbulent motion. J. Fluid Mech., 3, 4, 418–436, 1958.

[29]   Yang, K.; Pan, T.; Lei, Q.; Dong, X.; Cheng, Q.; Han, Y. A Roadmap to Sorption-Based Atmospheric Water Harvesting: From Molecular Sorption Mechanism to Sorbent Design and System Optimization. Environ. Sci. Technol., 2021.

[30]   Kim, H.; Rao, S. R.; Kapustin, E. A.; Zhao, L.; Yang, S.; Yaghi, O. M.; Wang, E. N. Adsorption-based atmospheric water harvesting device for arid climates. Nat. Commun., 9, 1, 1–8, 2018.

[31]   Xu, Y.; Wang, X.; Zhou, J.; Song, B.; Jiang, Z.; Lee, E. M.Y.; Huberman, S.; Gleason, K. K.; Chen, G. Molecular engineered conjugated polymer with high thermal conductivity. Sci. Adv., 4, 3, 1–7, 2018.

[32]   Legrand, U.; Castillo Sánchez, J. R.; Boudreault, R.; Meunier, J.-L.; Girard Lauriault, P.-L.; Tavares, J. R. Fundamental thermodynamic properties of sorbents for atmospheric water capture. Chem. Eng. J., 431, 2, 134058, 2022.

[33]   Chakraborty, A.; Saha, B. B.; Koyama, S.; Ng, K. C.; Srinivasan, K. Adsorption thermodynamics of silica gel-water systems. J. Chem. Eng. Data, 54, 2, 448–452, 2009.

[34]   Sharafian, A.; Fayazmanesh, K.; McCague, C.; Bahrami, M. Thermal conductivity and contact resistance of mesoporous silica gel adsorbents bound with polyvinylpyrrolidone in contact with a metallic substrate for adsorption cooling system applications. Int. J. Heat Mass Transf., 79, 64–71, 2014.

[35]   Islam, M. A.; Thu, K.; Saha, B. B. Specific heat capacity of mesoporous silica gel for adsorption heat pump applications. Nov. Carbon Sci. Green Asia Strateg., 19, 2017, [Online]. Available: http://www.tj.kyushu-u.ac.jp/leading/pdf/06-2017Seminar-Proceedings_P19.pdf (accessed Jul. 20, 2021).

[36]   Laybourn, A.; Katrib, J.; Ferrari-John, R. S.; Morris, C. G.; Yang, S.; Udoudo, O.; Easun, T. L.; Dodds, C.; Champness, N. R.; Kingman, S. W.; Schröder, M. Metal-organic frameworks in seconds via selective microwave heating. J. Mater. Chem. A, 5, 16, 7333–7338, 2017.

[37]   Huber, L.; Ruch, P.; Hauert, R.; Matam, S. K.; Saucke, G.; Yoon, S.; Zhang, Y.; Koebel, M. M. Water sorption behavior of physically and chemically activated monolithic nitrogen doped carbon for adsorption cooling. RSC Adv., 6, 84, 80729–80738, 2016.

[38]   LaPotin A.; Zhong, Y.; Zhang, L.; Zhao, L.; Leroy, A.; Kim, H.; Rao, S. R.; Wang, E. N. Dual-Stage Atmospheric Water Harvesting Device for Scalable Solar-Driven Water Production. Joule, 5, 1, 166–182, 2021.

[39]   LaPotin, A.; Kim, H.; Rao, S. R.; Wang, E. N. Adsorption-Based Atmospheric Water Harvesting: Impact of Material and Component Properties on System-Level Performance. Acc. Chem. Res., 52, 6, 1588–1597, 2019.

[40]   Van Heyden, H.; Munz, G.; Schnabel, L.; Schmidt, F.; Mintova, S.; Bein, T. Kinetics of water adsorption in microporous aluminophosphate layers for regenerative heat exchangers. Appl. Therm. Eng., 29, 8–9, 1514–1522, 2009.

[41]   Hanikel, N.; Prévot, M. S.; Fathieh, F.; Kapustin, E. A.; Lyu, H.; Wang, H.; Diercks, N. J.; Glover, T. G.; Yaghi, O. M. Rapid Cycling and Exceptional Yield in a Metal-Organic Framework Water Harvester. ACS Cent. Sci., 5, 10, 1699–1706, 2019.

[42]   Hossain, M. I.; Glover, T. G. Kinetics of Water Adsorption in UiO-66 MOF. Ind. Eng.

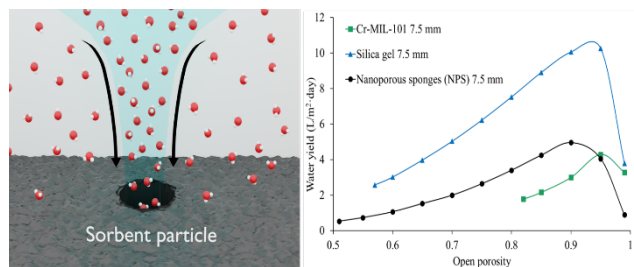Chem. Res., 58, 24, 10550–10558, 2019.

Table of content graphic:

Table of Content text:

The water sorption kinetics of silica gel, a MOF and a synthesized carbon-based material have been determined experimentally and theoretically for thick powder layers. Open porosity, i.e. the amount of void in a layer was the most important parameter influencing kinetics. The maximum water uptake and the kinetics of single particle were not necessarily predictive of the water capture performance.